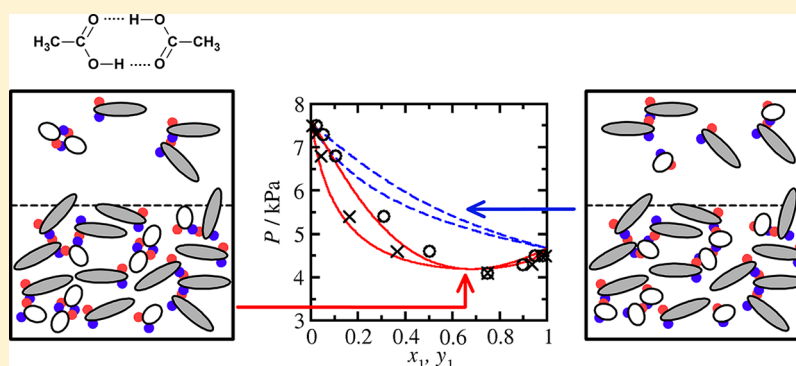


## Influence of Cyclic Dimer Formation on the Phase Behavior of Carboxylic Acids. II. Cross-Associating Systems

Jiří Janeček<sup>†,‡</sup> and Patrice Paricaud<sup>\*,‡</sup><sup>†</sup>Mines ParisTech, CTP, 35 rue saint Honoré 77305 Fontainebleau Cedex, France<sup>‡</sup>ENSTA-ParisTech, UCP, 828 Boulevard des Maréchaux, 91762 Palaiseau Cedex, France

## S Supporting Information



**ABSTRACT:** The doubly bonded dimer association scheme (DBD) proposed by Sear and Jackson is extended to mixtures exhibiting both self- and cross-associations. The PC-SAFT equation of state is combined with the new DBD association contribution to describe the vapor–liquid equilibria of binary mixtures of carboxylic acids + associating compounds (water, alcohols, and carboxylic acids). The effect of doubly bonded dimers on the phase behavior in such systems is less important than in mixtures of carboxylic acids with nonassociating compounds, due to the cross-associations that compete with the formation of DBDs. Nevertheless, a clear improvement in the description of vapor–liquid coexistence curves is achieved over the classical 2B association model, particularly for the dew point curves.

## 1. INTRODUCTION

Carboxylic acids are important chemicals encountered in many different areas of the chemical industry. They are used in the production of polymers, pharmaceutical compounds, biofuels, solvents, paints, and food additives. Short acids have a broad range of applications: acetic acid is a raw material for the production of vinyl acetate monomer and acetic anhydride. Acrylic and metacrylic acids are also precursors of polymers and adhesives. Fatty acids play an important role in the production of biofuels: biodiesels are prepared by the transesterification of oils that are mainly composed of carboxylic acids. Mixtures of carboxylic acids and other polar compounds such as water, alcohols, and esters are often encountered in chemical processes: the transesterification reaction involves water, an alcohol, an ester, and a carboxylic acid. It is important to know the thermodynamic properties and the phase behavior of such mixtures to design the separation units of the process. For instance, the design of a distillation column requires an accurate model knowledge for the vapor–liquid equilibria (VLE) and enthalpies of vaporization.

It is well-known that short carboxylic acids dimerize in the vapor phase,<sup>1</sup> giving rise to a low vapor phase compressibility factor and a low vaporization enthalpy. Equations of state that do not take the dimerization into account largely overestimate

the vaporization enthalpy of pure carboxylic acids. The vapor–liquid phase equilibria of mixtures of carboxylic acids has been often modeled with an activity coefficient model for the liquid phase combined with the Hayden–O’Connell<sup>2</sup> model, which takes the dimerization in the vapor phase into account. Although this approach can lead to an accurate description of the VLE of mixtures at low pressures, it cannot accurately predict liquid densities, and does not take cross-associations into account.

The statistical association fluid theory<sup>3–5</sup> (SAFT) is a molecular based equation of state (EoS) that takes the formation of hydrogen bonds into account through Wertheim’s TPT1 association theory.<sup>6–10</sup> Two association schemes (1A and 2B) are usually considered to describe hydrogen bonding in carboxylic acid systems: the 1A association scheme considers a single association site A on the carboxylic acid molecule, which can bond to another site of the same type on another molecule; the classical 2B association scheme considers two different sites A and B on the molecules, which only form A–B bonds but no doubly bonded dimers (DBD). The 1A

Received: February 2, 2013

Revised: June 27, 2013

Published: June 27, 2013

association model well describes the behavior of carboxylic acids in vapor phases where a high fraction of molecules forms doubly bonded dimers. However, the 1A association scheme cannot describe the formation of chain-like aggregates in liquid phases rich in acid molecules. Despite this lack, the 1A model was adopted for carboxylic acids by most authors. The reader is directed to an excellent review by Breil et al.<sup>11</sup> of the modeling studies of carboxylic acids using SAFT-like models. Lymperiadis et al.<sup>12</sup> developed a group contribution method within the SAFT- $\gamma$  approach and used the 1A association scheme for carboxylic acids; dos Ramos et al.<sup>13</sup> also developed a group contribution method for acids within the GC-SAFT-VR approach, by considering an asymmetric association scheme with one donor site and three acceptor sites. Recently, Chen et al. employed the PC-SAFT EoS with the 2B association model to describe phase equilibria of mixtures containing acetic, propionic, and acrylic acids.<sup>14</sup> Piazza and Span<sup>15</sup> suggested a multiparameter equation of state for acetic acid based on SAFT, which correlates a broad range of properties over wide ranges of conditions with high accuracy. Breil et al.<sup>11</sup> were able to accurately represent the thermodynamic properties (including vaporization enthalpies) of pure acetic acid and mixtures using the cubic plus association (CPA) EoS + 1A model. Derawi et al.<sup>16</sup> compared the 1A and 2B association schemes using the CPA equation of state, and found that the 1A model gives rise to better results for binary systems. Soo<sup>17</sup> performed an extensive modeling study of mixtures of carboxylic acids with polar and nonpolar compounds, and compared different versions of the PC-SAFT EoS combined with the 1A association scheme. He managed to obtain an excellent description of the experimental data by using an additional binary parameter in the dispersion term of PC-SAFT.

We have recently proposed the PC-SAFT-DBD model<sup>18</sup> based on a combination of the doubly bonded dimer association scheme of Sear and Jackson<sup>19</sup> with the PC-SAFT equation of state.<sup>20,21</sup> The PC-SAFT-DBD model can accurately describe the phase behavior for pure carboxylic acids and binary mixtures of an acid with an alkane. The doubly bonded dimers association scheme (DBD) is an extension of the classical 2B association model,<sup>22,23</sup> and takes into account the formation of chain-like clusters as well as the formation of cyclic dimers. Such dimers cannot further associate. As shown in our previous work,<sup>18</sup> the formation of dimers induces a lower molar volume in the gas phase, leading to a lower vaporization enthalpy according to Clapeyron's thermodynamic law when vapor pressures are regressed. The new DBD model can accurately describe the experimental vapor pressures, coexistence densities, and vaporization enthalpies of pure carboxylic acids, and leads to a better description of the VLE of mixtures than the 1A and 2B association schemes. In the current work, we propose an extension of the DBD model to cross-associating systems of carboxylic acids, alcohols, and water.

## 2. THEORY

We consider a multicomponent system of  $n$  associating compounds that may form DBDs. Each molecule  $i$  has two associating sites: one acceptor  $A_i$  site and one donor  $B_i$ . The molecules can form simple  $A-B$  bonds and doubly bonded dimers. The association contribution  $A^{\text{assoc}}$  of the Helmholtz free energy of this mixture is given by<sup>19,24</sup>

$$\frac{A^{\text{assoc}}}{Vk_B T} = \sum_i \left( \sigma_{\Gamma_i} \ln \frac{\sigma_{0_i}}{\sigma_{\Gamma_i}} + \sigma_{\Gamma_i} - \sigma_{A_i} - \sigma_{B_i} + \frac{\sigma_{A_i} \sigma_{B_i}}{\sigma_{0_i}} \right) - \sum_i \sum_j \sigma_{A_i} \sigma_{B_j} \Delta_{A_i B_j} - \frac{1}{2} \sum_i \sum_j \sigma_{0_i} \sigma_{0_j} \Phi_{ij} \quad (1)$$

where  $V$  is the volume of the system,  $T$  the temperature, and  $k_B$  the Boltzmann constant;  $\sigma_{A_i}$  is the number density of molecules  $i$  with site  $A_i$  nonbonded (analogously  $\sigma_{B_i}$ ), and  $\sigma_{0_i}$  is the number density of molecules  $i$  with both association sites nonbonded;  $\sigma_{\Gamma_i} = \rho x_i$  denotes the number density of component  $i$ ;  $\rho$  is the total number density of the mixture, and  $x_i$  is the molar fraction of component  $i$ . We used here Wertheim's formalism for the number densities  $\sigma_{A_i}$  that should not be confused with the segment diameters  $\sigma_i$ . All summations run over all the  $n$  components of the mixture. The association strength  $\Delta_{A_i B_j}$  is approximated in the same way as in the classical SAFT approach, as

$$\Delta_{A_i B_j} = \kappa_{A_i B_j} g_c(d_{ij}) \sigma_{ij}^3 \left[ \exp\left(\frac{\epsilon_{A_i B_j}}{k_B T}\right) - 1 \right] \quad (2)$$

In this work,  $\sigma_{ij}$  is the cross-interaction diameter between spherical segments  $i$  and  $j$  and should not be confused with the number densities of nonbonded molecules. The bonding energy  $\epsilon_{A_i B_j}$  and bonding volume  $\kappa_{A_i B_j}$  are the association parameters of pure component  $i$ ;  $g_c(d_{ij})$  is the contact value of the radial distribution function between the spherical segments of chains  $i$  and  $j$ , which is approximated by the contact value for the hard sphere mixture. The cross-bonding energy and cross-bonding volume are estimated with the combining rule of Wolbach and Sander,<sup>25</sup> which is given by

$$\epsilon_{A_i B_j} = 0.5(\epsilon_{A_i B_i} + \epsilon_{A_j B_j}) \quad (3)$$

and

$$\kappa_{A_i B_j} = \sqrt{\kappa_{A_i B_i} \kappa_{A_j B_j}} \left( \frac{\sqrt{\sigma_{ii} \sigma_{jj}}}{0.5(\sigma_{ii} + \sigma_{jj})} \right)^3 \quad (4)$$

The association parameters between different molecules are symmetric: for the ethanol–acetic acid mixture, the bonding energy  $\epsilon_{A_i B_j}$  is the same when ethanol serves as the hydrogen bond donor or acceptor and the same holds for the bonding volume  $\kappa_{A_i B_j}$ . The integral that corresponds to the formation of doubly bonded dimers  $\Phi_{ij}$  for molecules of different compounds can be expressed as

$$\Phi_{ij} = \kappa_{A_i B_j} g_c(d_{ij}) \sigma_{ij}^3 \left[ \exp\left(\frac{\epsilon_{A_i B_j}}{k_B T}\right) - 1 \right] \left[ \exp\left(\frac{\epsilon_{A_j B_i}}{k_B T}\right) - 1 \right] f_v^{ij} \quad (5)$$

Note that the Mayer functions in eq 5 are identical, since  $\epsilon_{A_i B_j} = \epsilon_{A_j B_i}$ . The parameter  $f_v^{ij}$  reflects the ability of molecules to form cyclic dimers. For DBDs between molecules of different compounds, we use the following combining rule

$$f_v^{ij} = \sqrt{f_v^{ii} f_v^{jj}} \quad (6)$$

For the compounds that do not form doubly bonded dimers alone (e.g., monofunctional alcohols or water within this work),

Table 1. List of Systems Studied in This Work<sup>a</sup>

	model	ARD <sub>0</sub> % (P/y)	$k_{ij}$	AD <sub>k</sub> % (P/y)
Methanol–Acetic Acid <sup>26</sup>				
$T = 308.15$ K	DBD	6.58/2.44	−0.01927	1.85/1.12(*)
	2B	10.7/6.50	−0.02877	1.58/4.04(*)
$T = 318.15$ K	DBD	6.56/2.72	−0.01938	3.09/1.53(*)
	2B	9.35/6.79	−0.03048	2.64/4.27(*)
Ethanol–Acetic Acid <sup>26,27</sup>				
$T = 308.15$ K	DBD	7.48/1.44	−0.01867	0.76/0.89(*)
	2B	13.8/5.91	−0.03638	1.45/1.53(*)
$T = 318.15$ K	DBD	8.51/1.86	−0.02026	1.12/0.78(*)
	2B	14.7/6.08	−0.03965	1.35/1.59(*)
$P = 101.3$ kPa	DBD	13.8/2.72(*)	−0.04157	2.66/2.17
	2B	19.5/5.39(*)	−0.06072	2.61/1.35
Ethanol–Propionic Acid <sup>28</sup>				
$T = 323.2$ K	DBD	3.16/0.93	−0.00490	3.15/1.29(*)
	2B	4.08/2.94	−0.00475	4.06/2.39(*)
1-Butanol–Acetic Acid <sup>28</sup>				
$T = 323.2$ K	DBD	2.70/1.07	+0.00740	1.93/0.75
	2B	10.1/3.20	−0.03977	2.57/1.54
Acetic Acid–Propionic Acid <sup>29</sup>				
$T = 323.2$ K	DBD	3.33/6.01	+0.01017	0.98/0.22
	1A	2.05/2.85	+0.00277	1.22/3.38
	2B	2.14/3.84	+0.00498	1.69/4.09
Formic Acid–Propionic Acid <sup>29</sup>				
$T = 343.2$ K	DBD	9.67/2.55	+0.03521	1.16/1.00
	1A	7.50/4.37	+0.02214	1.20/5.26
	2B	7.50/5.01	+0.03298	1.83/7.02
Propionic Acid–Water <sup>30</sup>				
$P = 101.3$ kPa	DBD+2B	8.60/4.90(*)	−0.02821	5.36/3.21
	2B+2B	9.89/5.07(*)	−0.03040	6.40/2.92
	DBD+4C	31.6/15.3(*)	−0.09560	2.64/1.90
	2B+4C	30.0/13.4(*)	−0.1057	3.33/1.96
Acetic Acid–Water <sup>30</sup>				
$P = 101.3$ kPa	DBD+4C	29.7/13.0(*)	−0.1178	1.28/0.92
	2B+4C	36.1/14.9(*)	−0.1472	0.93/1.58
$P = 26.67$ kPa	DBD+4C	38.6/15.0(*)	−0.1148	2.13/1.18
	2B+4C	44.6/16.7(*)	−0.1404	2.16/2.42
$P = 9.333$ kPa	DBD+4C	46.0/17.3(*)	−0.1154	1.87/1.41
	2B+4C	51.4/18.0(*)	−0.1454	2.04/2.26

<sup>a</sup>The first column corresponds to the average relative deviations (ARDs) for pressures and vapor phase mole fractions obtained with  $k_{ij} = 0$ ; the last column contains deviations calculated with an optimized binary parameter given in the third column of the table. The items denoted by an asterisk are not shown in any figure.

the parameter  $f_v$  vanishes and the square-root combining rule implies that such compounds do not participate on formation of cross-cyclic dimers neither with carboxylic acids. We note that the hydroxyl group (or the water molecule) can also form a cyclic associate with a carboxyl group; however, these species are of rather low importance with respect to their lower stability (compared to DBDs formed by two carboxylic groups) and concentration. For systems in which the formation of cyclic dimers is caused by more associating groups (like ethylene glycol), this simple combining rule may not be directly applicable. After some manipulation (see Appendix I in the Supporting Information), the association Helmholtz energy can be expressed in terms of the fractions of nonbonded species as

$$\frac{A^{\text{assoc}}}{Nk_B T} = \sum_i x_i \left( \ln X_{0i} - \frac{X_{A_i}}{2} - \frac{X_{B_i}}{2} + \frac{X_{A_i} X_{B_i}}{2X_{0i}} + \frac{1}{2} \right) \quad (7)$$

where  $X_{A_i} = \sigma_{A_i}/\sigma_{\Gamma_i}$  is the fraction of molecules  $i$  with  $A_i$  nonbonded,  $X_{B_i} = \sigma_{B_i}/\sigma_{\Gamma_i}$  the fraction of molecules  $i$  with  $B_i$  nonbonded, and  $X_{0i} = \sigma_{0i}/\sigma_{\Gamma_i}$  the fraction of molecules  $i$  nonbonded at both sites (i.e., the fraction of free molecules  $i$ ).

For an  $n$ -component mixture, the equilibrium composition of the associating system is given by the following set of  $3n$  equations, which are obtained by the minimization of the association Helmholtz energy with respect to  $\sigma_{A_k}$ ,  $\sigma_{B_k}$ , and  $\sigma_{0_k}$  for all components  $k$ :

$$\frac{X_{B_k}}{X_{0_k}} = 1 + \rho \sum_j x_j X_{B_j} \Delta_{A_k B_j} \quad (8)$$

$$\frac{X_{A_k}}{X_{0_k}} = 1 + \rho \sum_j x_j X_{A_j} \Delta_{A_j B_k} \quad (9)$$

$$0 = \frac{1}{X_{0k}} - \frac{X_{A_k}X_{B_k}}{X_{0k}^2} - \rho \sum_j x_j X_{0j} \Phi_{jk} \quad (10)$$

These equations are linked together by the summation terms on the right-hand sides. An iterative technique to solve this nonlinear system of equations is provided in Appendix II in the Supporting Information. If component  $k$  does not associate, the association strengths  $\Delta_{A_kB_j}$  as well as the integrals  $\Phi_{kj}$  vanish. Such nonassociating compounds indirectly affect the association equilibria by decreasing the mole fractions of the associating components. If component  $k$  can be associated but does not form DBD (i.e., if  $f_v^{kk} = 0$  like for alcohols), the third equation turns into the relation for the classical 2B model. In such a case,  $X_{0k} = X_{A_k}X_{B_k}$  and the first two equations become identical with the conditions for fractions of nonbonded sites as used in the classical SAFT approach.

In this work, the DBD association scheme is employed with the original version of the perturbed chain SAFT EoS (PC-SAFT).<sup>20,21</sup> The PC-SAFT model takes the repulsion, dispersion, and association interactions into account, while the dipolar, quadrupolar, or polarization contributions are not explicitly considered. The mixing rules given by Gross and Sadowski<sup>20,21</sup> are used in this work. To improve the description in some cases, we had to consider a binary parameter  $k_{ij}$  that modifies the energy parameter of cross-dispersion interactions as  $\varepsilon_{ij} = (1 - k_{ij})(\varepsilon_{ii}\varepsilon_{jj})^{1/2}$ .

### 3. RESULTS

The new PC-SAFT-DBD EoS is applied to several binary mixtures of carboxylic acids with alcohols, water, and other carboxylic acids. The results obtained with the PC-SAFT-DBD model are compared with those obtained with PC-SAFT combined with the classical 2B association scheme. In the case of mixtures of two different carboxylic acids, the 1A association scheme is also considered. The 1A model was not used for mixtures either with alcohols or with water, because it is not clear how to determine the cross-association energy and bonding volume between the carboxylic acid molecule and an alcohol or water molecule, since the single A site on the carboxylic acid molecule describes both the donor and acceptor sites.

The considered systems are listed in Table 1 together with the average deviations in pressure and vapor phase composition, and with the values of the binary mixing parameters  $k_{ij}$ . The binary mixing parameters were determined by minimizing the sum of the squared relative deviations between the calculated and experimental boiling pressures; the experimental vapor compositions were not used in the optimizing process, and the deviations are shown only for comparison. The PC-SAFT parameters of 2B models for alcohols and water are taken from Gross and Sadowski,<sup>20</sup> and those for the carboxylic acids are taken from our previous work.<sup>18</sup>

For binary mixtures of a carboxylic acid (2) and another associating compound (1) such as an alcohol or water, doubly bonded dimers are formed only between two molecules of carboxylic acids. The set of equilibrium conditions for the fractions of nonbonded sites (eqs 8–10) reduces to

$$\frac{1}{X_{A_1}} = 1 + \rho x_1 X_{B_1} \Delta_{11} + \rho x_2 X_{B_2} \Delta_{12} \quad (11)$$

$$\frac{X_{B_2}}{X_{0_2}} = 1 + \rho x_1 X_{B_1} \Delta_{21} + \rho x_2 X_{B_2} \Delta_{22} \quad (12)$$

$$0 = \frac{1}{X_{0_2}} - \frac{X_{A_2}X_{B_2}}{X_{0_2}^2} - \rho x_2 X_{0_2} \Phi_{22} \quad (13)$$

with  $X_{A_1} = X_{B_1}$  and  $X_{A_2} = X_{B_2}$ . A simplified notation for the association strength,  $\Delta_{12} \equiv \Delta_{A_1B_2} = \Delta_{A_2B_1}$ , is used.

The VLE curves of the methanol (1)–acetic acid (2) mixture at  $T = 308.15$  K (upper plot) and  $T = 318.15$  K (lower plot) calculated using the PC-SAFT-DBD model (solid black lines) and PC-SAFT-2B model (dashed red lines) are compared with experimental data<sup>26</sup> in Figure 1. A very good prediction of the

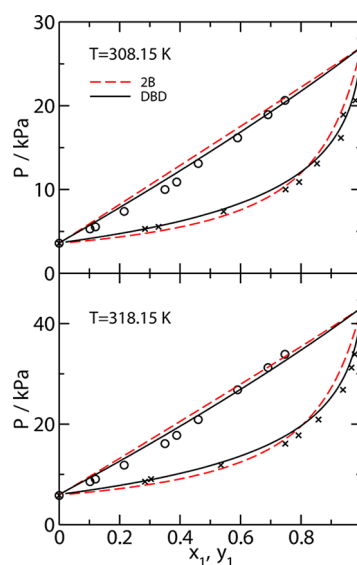


**Figure 1.** Vapor–liquid equilibria of the methanol (1)–acetic acid (2) mixture at  $T = 308.15$  K (upper graph) and  $T = 318.15$  K (lower graph). The solid black lines are the prediction obtained with the DBD association scheme; the red dashed lines are calculated with the classical 2B model. In both cases,  $k_{ij} = 0$ . The symbols denote the experimental data from ref 26.

VLE curves with  $k_{ij} = 0$  is obtained with both association schemes, showing that the association interactions are predominant and that the Wolbach and Sander combining rule<sup>25</sup> leads to good predictions. Here, the effect of the formation of doubly bonded dimers is limited and the mixture behaves almost as an ideal solution, as methanol molecules strongly associate with acetic acid molecules. As a result, the formation of doubly bonded dimers is low in the liquid phase and the content of chain-like structures is high. Thus, the DBD scheme does not bring a significant improvement over the 2B model for the description of the bubble point curve. However, the formation of cyclic dimers of acetic acid remains important in the vapor phase and the use of the DBD association scheme improves the description of the dew point curve. The agreement between the experimental data<sup>26</sup> and the PC-SAFT EoS prediction is slightly worse for the ethanol (1)–acetic acid (2) mixture, as shown in Figure 2. One can observe that the mixture significantly deviates from the ideal solution. In this case, we can also observe a shift of the dew point curve to higher pressures when the DBD scheme is used. The data of Table 1 indicate that the used optimized binary mixing parameters lead to a reduction of deviations in pressure for



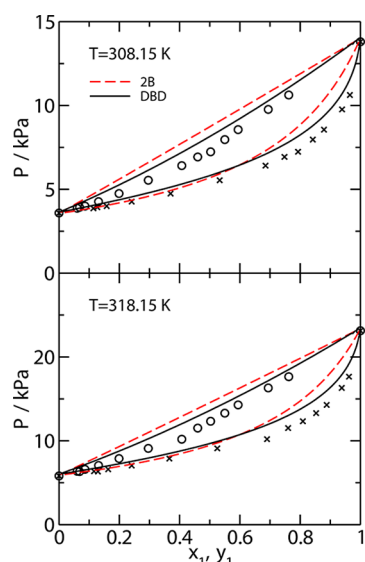


**Figure 2.** Vapor–liquid equilibria of the ethanol (1)–acetic acid (2) mixture at  $T = 308.15$  K (upper graph) and  $T = 318.15$  K (lower graph). The meaning of the lines is the same as that in Figure 1. The symbols denote the experimental data from ref 26.

both association schemes. However, the DBD model can better describe the dew point curve. The temperature difference between the two sets (for both previous systems) is rather small. To compare the performance of the two association schemes at higher temperature, we show isobaric VLE for the system ethanol–acetic acid at  $P = 101.3$  kPa<sup>27</sup> in Figure 3; this

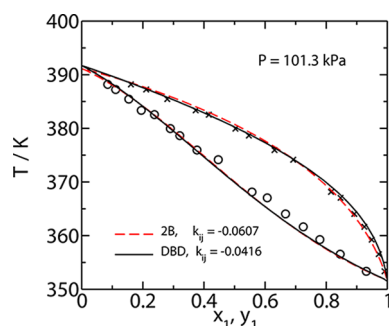


**Figure 3.** Isobaric VLE for the ethanol (1)–acetic acid (2) binary mixture at  $P = 101.3$  kPa. The lines show the 2B (red dashed) and DBD distillation curves calculated with the corresponding binary mixing parameters, and the symbols denote the experimental data from ref 27.

system is the only one treated in this work, for which the 2B model works better than DBD in pressure as well as in vapor composition. The corresponding values of  $k_{ij}$  are significantly different from the values obtained at  $T = 308.15$  K and  $T = 318.15$  K for both association models. The VLE curve of the ethanol (1)–propionic acid (2) mixture at  $T = 343.2$  K is very well predicted with the PC-SAFT-DBD model, as shown in Figure 4. In general, the DBD association scheme helps in improving the description of the dew point curves compared to the 2B model for carboxylic acids + short alcohol mixtures. The mixtures of carboxylic acids with longer alcohols exhibit a higher degree of nonideality. An example is the mixture 1-butanol (1)–acetic acid (2) at  $T = 323.2$  K shown in Figure 5.<sup>28</sup> In this figure, the upper graph corresponds to the

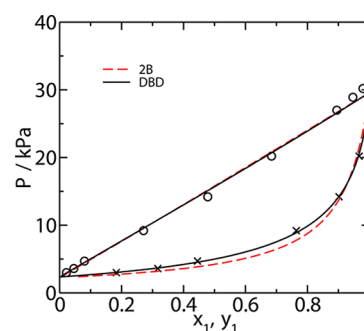


**Figure 4.** Vapor–liquid equilibria of the ethanol (1)–propionic acid (2) mixture at  $T = 323.2$  K. The lines have the same meaning as in Figure 1. The symbols denote the experimental data from ref 28.

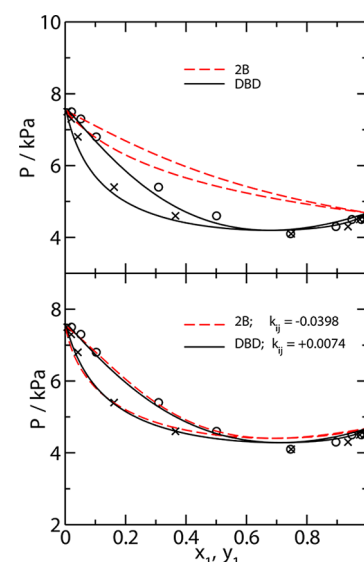


**Figure 5.** Vapor–liquid equilibria of the *n*-butanol (1)–acetic acid (2) mixture at  $T = 323.2$  K. The upper graph corresponds to the predictions of PC-SAFT with the DBD (solid black line) and 2B association models (dashed red line) with  $k_{ij} = 0$ , and the lower graph corresponds to the same calculation with  $k_{ij}$  fitted to the experimental data of ref 28 (symbols).

predictions of VLE with  $k_{ij} = 0$ , and the lower one corresponds to the phase diagram calculated with a binary parameter  $k_{ij}$  fitted to bubble pressures. The DBD model estimates the azeotropic composition and pressure surprisingly well even with  $k_{ij} = 0$ .

For binary mixtures of two carboxylic acids, two separate conditions have to be considered for  $X_{01}$  and  $X_{02}$ , and the following set of four equations must be solved:

$$\frac{X_{B1}}{X_{01}} = 1 + \rho x_1 X_{B1} \Delta_{11} + \rho x_2 X_{B2} \Delta_{12} \quad (14)$$

$$\frac{X_{B2}}{X_{02}} = 1 + \rho x_1 X_{B1} \Delta_{21} + \rho x_2 X_{B2} \Delta_{22} \quad (15)$$

$$0 = \frac{1}{X_{01}} - \frac{X_{A1} X_{B1}}{X_{01}^2} - \rho x_1 X_{01} \Phi_{11} - \rho x_2 X_{02} \Phi_{12} \quad (16)$$

$$0 = \frac{1}{X_{02}} - \frac{X_{A2} X_{B2}}{X_{02}^2} - \rho x_2 X_{02} \Phi_{22} - \rho x_1 X_{01} \Phi_{21} \quad (17)$$

The VLE for acetic acid (1)–propionic acid (2) at  $T = 343.2$  K is shown in Figure 6.<sup>29</sup> This mixture behaves as an ideal

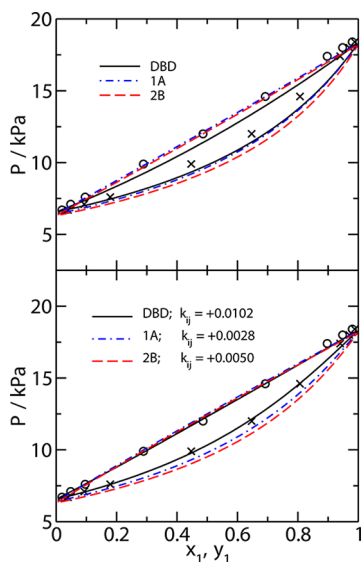


**Figure 6.** Vapor–liquid equilibria of the acetic acid (1)–propionic acid (2) mixture at  $T = 343.2$  K. The upper graph corresponds to the predictions of PC-SAFT with the DBD (solid black line), 2B (dashed red line), and 1A association models (blue, dash-dotted line) with  $k_{ij} = 0$ , and the lower graph corresponds to the same calculations with  $k_{ij}$  fitted to the experimental data from ref 29 (symbols).

solution as the interactions between like and unlike species are similar. The upper graph of Figure 6 corresponds to predictions obtained with  $k_{ij} = 0$ , and the lower graph corresponds to a description of the experimental data with a single binary parameter  $k_{ij}$  optimized to the bubble pressures. Although the two classical association models (1A and 2B) match the boiling point curve with  $k_{ij} = 0$  almost perfectly, the content of the most volatile component (acetic acid) in the vapor phase is overestimated. The DBD association scheme enables the experimental data to be matched almost perfectly when a single binary parameter is employed. Similar observations can be made for the phase diagram of the formic acid (1)–propionic acid (2) mixture at  $T = 343.2$  K, which is shown in Figure 7.<sup>29</sup> Interestingly, the curves calculated using the 1A scheme have reasonable course, despite the value of the bonding volume for formic acid reported in our previous work<sup>18</sup> ( $\kappa = 5.503$ ), which seems too large. These two systems illustrate the most important feature of the DBD association scheme. While the two classical models predict the phase diagrams too “broad” (the fraction of the more volatile component in the vapor phase is too high), in the case of the DBD scheme, the phase diagrams are more narrow. Thus, the shift of phase diagram with a nonzero  $k_{ij}$  (toward higher pressures in these two cases) may result in a perfect fit of both branches by the DBD scheme. Chen et al.<sup>14</sup> observed the same effect for isobaric VLEs of mixtures of acetic acid–acrylic acid and acetic acid–propionic acid.

We have chosen the system propionic acid (1)–water (2) at  $P = 101.325$  kPa<sup>30</sup> as an example of aqueous mixtures. The corresponding phase diagrams are depicted in Figure 8. We have first considered the 2B model for water with the parameters reported by Gross and Sadowski.<sup>20</sup> The calculations with this water model are performed in the same way as those for alcohol–acid mixtures, using eqs 1 and 13. Despite that the

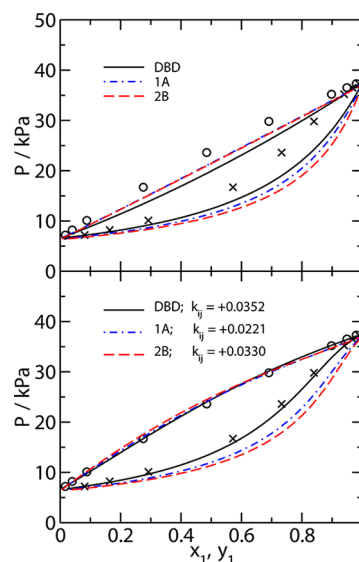


**Figure 7.** Vapor–liquid equilibria of the formic acid (1)–propionic acid (2) mixture at  $T = 343.2$  K. The upper graph corresponds to the predictions of PC-SAFT with the DBD (solid black line), 2B (dashed red line), and 1A association models (blue, dash-dotted line) with  $k_{ij} = 0$ , and the lower graph corresponds to the same calculations with  $k_{ij}$  fitted to the experimental data from ref 29 (symbols).

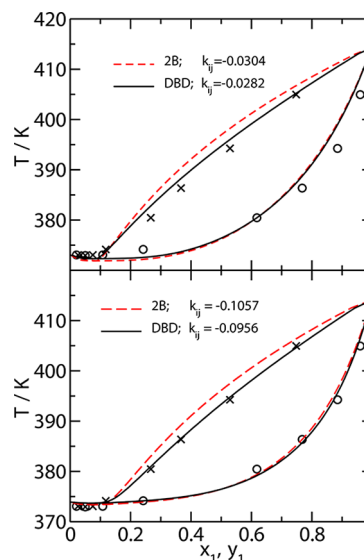


**Figure 8.** Vapor–liquid equilibria of the propionic acid (1)–water (2) binary mixture at  $P = 101.325$  kPa. The symbols denote the experimental data from ref 30. The upper graph corresponds to calculations with PC-SAFT + DBD (solid black line) and PC-SAFT + 2B (dashed red line) by using a binary parameter and a 2B model for water, and the lower graph corresponds to the same calculations with the 4C model for water and the third parameter set of Table 2.

DBD model (solid black lines) for propionic acid brings some improvement over the 2B model (dashed red line) in the description of the vapor phase composition, none of the models is able to accurately describe the course of the bubble point curve at high mole fractions of propionic acid.

We then considered a four-site model (4C model) for water, which has two hydrogen acceptors and two donors corresponding to the electron pairs of the oxygen atom. We have fixed the number of segments to  $m = 1.0$  and tried to fit the remaining four PC-SAFT parameters to vapor pressures

Table 2. Different Sets of PC-SAFT Parameters for Pure Water (Two-Site and Four-Site Models)<sup>a</sup>

	<i>m</i>	$\sigma$ (Å)	$\epsilon/k_B$ (K)	$\kappa_{\text{Assoc}}$	$\epsilon_{\text{Assoc}}/k_B$	ARD% ( $P_{\text{vap}}/\rho_l$ )
4C	1.00	3.013	44.38	0.0481	2357.1	3.41/0.35
4C	1.00	3.065	441.7	0.0213	1262.2	0.20/0.62
4C	1.00	3.0556	273.05	0.03515	1749.3	1.10/1.21
2B	1.0656	3.0007	366.51	0.034868	2500.7	1.88/6.83*

<sup>a</sup>For all models,  $m = 1$ . The first and second lines correspond to an optimization on the vapor pressures and liquid densities of pure water in the temperature range 275–450 K, and the third parameter set was obtained by simultaneous optimization on the vapor pressures and liquid densities of pure water and VLE data of the water–ethanol binary mixture for  $T$  between 303.15 and 363.15 K. The parameters of the 2B model from ref 20 are reported in the last row; average relative deviations (ARDs) for pure water are also reported.

and saturated liquid densities in the temperature range 275–450 K. We found two different possible sets of parameters, one of them with a very low value of the dispersion parameter,  $\epsilon/k_B = 44.38$  K, and the second with a rather high value,  $\epsilon/k_B = 441.7$  K. Since none of the parameter sets led to a good description of the VLE of binary systems, we performed a reoptimization of the parameters for water by including VLE data of the ethanol–water mixture at  $T = 303.15$ , 323.15, 343.15, and 363.15 K.<sup>31</sup> The three parameter sets for the 4C model of pure water are compared in Table 2. Expectably, lowering the dispersion contribution to Helmholtz energy (i.e., the value of  $\epsilon$ ) leads to an increase of importance of the association contribution (increase of  $\epsilon_{\text{Assoc}}$ ). The parameter  $\sigma$  is rather unaffected, which was expected as the effect of this parameter on the liquid density can be hardly compensated by any change of the remaining parameters, if the number of segments  $m$  is fixed. Note that we did not include spectroscopy data in the optimization procedure like it was done by other authors, as the nonpolar PC-SAFT molecular model of water is not realistic enough to describe many properties simultaneously, and we focus here on phase equilibria. The use of the 4C model for water requires the modification of the association contribution to the Helmholtz energy. For a mixture of a carboxylic acid (1) and a 4C model for water (2), the association contribution can be written as

$$\frac{A^{\text{assoc}}}{Nk_B T} = x_1 \left( \ln X_{0_1} - \frac{X_{A_1}}{2} - \frac{X_{B_1}}{2} + \frac{X_{A_1}X_{B_1}}{2X_{0_1}} + \frac{1}{2} \right) + x_2 (2 \ln X_{A_2} + 2 \ln X_{B_2} - X_{A_2} - X_{B_2} + 2) \quad (18)$$

The set of equilibrium conditions for the fractions of nonbonded sites becomes

$$\frac{X_{B_1}}{X_{0_1}} = 1 + \rho x_1 X_{B_1} \Delta_{12} + 2\rho x_2 X_{B_2} \Delta_{11} \quad (19)$$

$$\frac{1}{X_{A_2}} = 1 + \rho x_1 X_{B_1} \Delta_{21} + 2\rho x_2 X_{B_2} \Delta_{22} \quad (20)$$

$$0 = \frac{1}{X_{0_1}} - \frac{X_{A_1}X_{B_1}}{X_{0_1}^2} - \rho x_1 X_{0_1} \Phi_{11} \quad (21)$$

The introduction of the 4C model for water with the third parameter set of Table 2 improves the description of the bubble point curve for both the 2B and DBD models of propionic acid. Although the numerical values of the average deviations reported in Table 1 are of comparable size for both models, the better performance of the DBD scheme is evident from Figure 9 (in this case, the average deviations are strongly affected by the three points between pure water and azeotropic

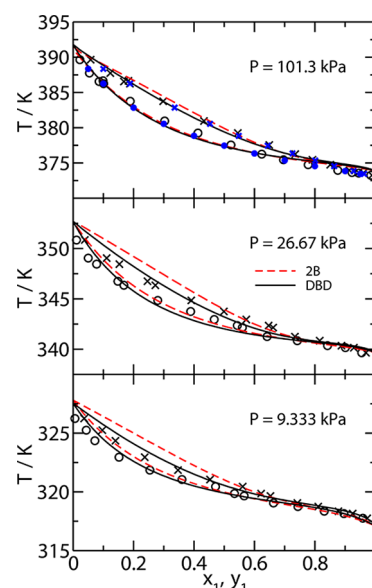


**Figure 9.** Vapor–liquid equilibria of the acetic acid (1)–water (2) binary mixtures at  $P = 101.3$  kPa (upper part),  $P = 26.67$  kPa (middle part), and  $P = 9.333$  kPa (lower part). The black symbols denote the experimental data from ref 30. The blue symbols for  $P = 101.3$  kPa are the experimental data of ref 32. The DBD (solid black) and 2B (dashed red) models are combined with the 4C model of water and the third parameter set of Table 2.

point). Thus, a very accurate description of VLE data can be obtained with a proper description of hydrogen bonding for both compounds.

In Figure 9, we compare the description of isobaric phase diagrams of the system water (1) + acetic acid (2) obtained with the 2B and DBD models. In this figure, only the 4C model for water is considered; the values of the corresponding  $k_{ij}$  are reported in Table 1. The experimental data are those of Ito et al.<sup>30</sup> for the highest pressure supplemented by those of Ramalho et al.<sup>32</sup> As in all previous cases, the DBD model leads to a better description of the vapor phase composition.

We can now discuss the formation of doubly bonded dimers in mixtures of carboxylic acids with polar and cross-associating molecules, and compare it to the formation of DBDs in carboxylic acids + nonpolar compound mixtures. The fractions of molecules of acetic acids bonded as DBDs ( $x_{\text{dd}} = 1 - (X_{A_1}X_{B_1}/X_{0_1})$ ) have been calculated with the PC-SAFT-DBD model for binary mixtures with *n*-octane at  $T = 343.15$  K ( $k_{ij} = +0.045$ ;<sup>18</sup> solid black curves in Figure 10) and with methanol at the same temperature ( $k_{ij} = -0.02$ ; red dashed curves in Figure 10).

The two upper curves (starting at  $x_{\text{dd}} \approx 0.8$  for  $x_1 = 0$ ) represent the content of DBDs in the vapor phases, while the

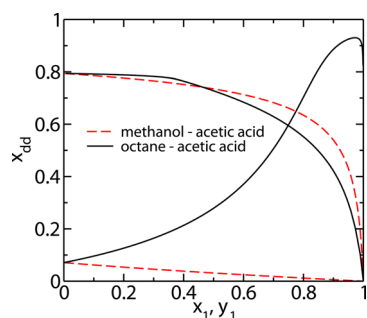


**Figure 10.** Fraction of acetic acid bonded as cyclic dimers in the coexisting vapor and liquid phases of the octane (1)–acetic acid (2) mixture at  $T = 343.15$  K (black lines) and of the methanol (1)–acetic acid (2) mixture at  $T = 343.15$  K (red dashed lines). The lower branches (starting at  $x_{dd} \approx 0.1$  for pure acetic acid,  $x_1 = 0$ ) correspond to the liquid phases, and the upper ones ( $x_{dd} \approx 0.9$ ), to the vapor phases.

two lower ones correspond to the liquid phases. For both systems, the molecules of acetic acid strongly associate as DBDs in the vapor phase up to high concentrations of the second component; when the molar fraction of acetic acid in the vapor phase becomes lower than  $x_2 \approx 0.1$ , the concentration of DBDs decays to zero. This can be explained by the decay of association between acetic acid molecules due to dilution; for the methanol–acetic acid mixture, this decay is enhanced by the formation of cross hydrogen bonds.

In the liquid phase of the acetic acid–methanol mixture, the content of DBDs decreases continuously from  $x_{dd} \approx 0.1$  for pure acetic acid to  $x_{dd} \approx 0$  at infinite dilution. This shows the importance of the competition between cross-associations and the formation of DBDs. In the case of the *n*-octane (1)–acetic acid (2) mixture, the fraction of DBDs increases as the *n*-octane mole fraction is increased in the liquid phase. This observation reflects an expectable fact: the less potential partners for hydrogen bonding the molecule of acid has, the higher is the probability to form a cyclic dimer. As a result, the use of DBDs has a much larger influence on the phase behavior for mixtures of carboxylic acids with nonassociating compounds than for mixtures of acids with cross-associating compounds.

#### 4. CONCLUSION

In this work, we extend the doubly bonded dimer (DBD) association scheme to mixtures of carboxylic acids and with other associating compounds. The DBD scheme is here combined with the PC-SAFT EoS. The DBD scheme leads to a significant improvement of the description of VLE data. In particular, the prediction of the vapor phase composition is dramatically improved. The formation of DBDs in mixtures with associating compounds plays a less important role because the cross-associations compete with the formation of DBDs between two acid molecules. As a result, the effect of DBDs on the phase behavior is less important in these mixtures than in mixtures of carboxylic acids with alkanes.<sup>18</sup>

The results presented in this work and in a previous article<sup>18</sup> intend to prove the superiority of the DBD model over the classical 1A and 2B models for carboxylic acids. While the 1A enables an adequate description of dimerization in the vapor phase and in liquid phases rich in nonpolar compounds, the 2B model enables a realistic description of liquid phases with alcohols and other associating compounds as it considers the formation of chain-like clusters. The DBD association scheme

is able to describe the features of both 1A and 2B models, by allowing the formation of chain-like structures in dense systems and of cyclic dimers in diluted phases. The main advantage of the new approach is the ability to correctly treat both liquid and vapor phases using only one expression for the association contribution, allowing the predictions of critical points. The new approach only requires one additional pure component parameter,  $f_v$ , which characterizes the ability of forming cyclic dimers. This parameter is correlated with the bonding energy and volume parameters, and several sets of parameters for a pure component can be found by fitting the pure component properties. However, all of these sets of pure component parameters may not lead to a good description of the phase behavior of mixtures. In a future work, we will discuss the effect of the  $f_v$  on the phase behavior of mixtures, in particular on liquid–liquid immiscibility.

#### ■ ASSOCIATED CONTENT

##### Supporting Information

More detailed derivation of eq 7 and relations for compression factor and composition derivatives of association Helmholtz energy are provided in Appendix I. An algorithm for searching the values of fractions of nonbonded sites is described in Appendix II. This material is available free of charge via the Internet at <http://pubs.acs.org>.

#### ■ AUTHOR INFORMATION

##### Corresponding Author

\*E-mail: [patrice.paricaud@ensta-paristech.fr](mailto:patrice.paricaud@ensta-paristech.fr).

##### Notes

The authors declare no competing financial interest.

#### ■ ACKNOWLEDGMENTS

The authors thank the financial support of the French Research National Agency (ANR-09-CP2D-10-03), as well as C. Coquelet from Mines-ParisTech. The access to the MetaCentrum computing facilities provided under the research intent MSM6383917201 is highly appreciated.

#### ■ REFERENCES

- (1) Miyamoto, S.; Nakamura, S.; Iwai, Y.; Arai, Y. Measurement of Vapor-Phase Compressibility Factors of Monocarboxylic Acids Using a Flow-Type Apparatus and Their Association Constants. *J. Chem. Eng. Data* **1999**, *44*, 48–51.
- (2) Hayden, J. G.; O'Connell, J. P. Generalized Method for Predicting 2nd Virial-Coefficients. *Ind. Eng. Chem. Process Des. Dev.* **1975**, *14*, 209–216.
- (3) Chapman, W.; Jackson, G.; Gubbins, K. Phase-Equilibria of Associating Fluids Chain Molecules with Multiple Bonding Sites. *Mol. Phys.* **1988**, *65*, 1057–1079.
- (4) Chapman, W. G.; Gubbins, K. E.; Jackson, G.; Radosz, M. SAFT: Equation-of-State Solution Model for Associating Fluids. *Fluid Phase Equilib.* **1989**, *52*, 31–38.
- (5) Chapman, W. G.; Gubbins, K. E.; Jackson, G.; Radosz, M. New Reference Equation of State for Associating Liquids. *Ind. Eng. Chem. Res.* **1990**, *29*, 1709–1721.
- (6) Wertheim, M. Fluids with Highly Directional Attractive Forces. I. Statistical Thermodynamics. *J. Stat. Phys.* **1984**, *35*, 19–34.
- (7) Wertheim, M. Fluids with Highly Directional Attractive Forces. II. Thermodynamic Perturbation Theory and Integral Equations. *J. Stat. Phys.* **1984**, *35*, 35–47.
- (8) Wertheim, M. Fluids with Highly Directional Attractive Forces. III. Multiple Attraction Sites. *J. Stat. Phys.* **1986**, *42*, 459–476.



- (9) Wertheim, M. Fluids with Highly Directional Attractive Forces. IV. Equilibrium Polymerization. *J. Stat. Phys.* **1986**, *42*, 477–492.
- (10) Wertheim, M. Fluids of Dimerizing Hard-Spheres, and Fluid Mixtures of Hard-Spheres and Dispheres. *J. Chem. Phys.* **1986**, *85*, 2929–2936.
- (11) Breil, M. P.; Kontogeorgis, G. M.; Behrens, P. K.; Michelsen, M. L. Modeling of the Thermodynamics of the Acetic Acid-Water Mixture Using the Cubic-Plus-Association Equation of State. *Ind. Eng. Chem. Res.* **2011**, *50*, 5795–5805.
- (12) Lympieriadis, A.; Adjiman, C. S.; Jackson, G.; Galindo, A. A Generalisation of the SAFT- Group Contribution Method for Groups Comprising Multiple Spherical Segments. *Fluid Phase Equilib.* **2008**, *274*, 85–104.
- (13) dos Ramos, M. C.; Haley, J. D.; Westwood, J. R.; McCabe, C. Extending the GC-SAFT-VR Approach to Associating Functional Groups: Alcohols, Aldehydes, Amines and Carboxylic Acids. *Fluid Phase Equilib.* **2011**, *306*, 97–111.
- (14) Chen, Y.; Attia, A.; Mutelet, F.; Solimando, R.; Mohamed, R. J. Thermodynamic Modeling of Mixtures Containing Carboxylic Acids Using the PC-SAFT Equation of State. *Ind. Eng. Chem. Res.* **2012**, *51*, 13846–13852.
- (15) Piazza, L.; Span, R. An Equation of State for Acetic Acid Including the Association Term of SAFT. *Fluid Phase Equilib.* **2011**, *303*, 134–149.
- (16) Derawi, S. O.; Zeuthen, J.; Michelsen, M. L.; Stenby, E. H.; Kontogeorgis, G. M. Application of the CPA Equation of State to Organic Acids. *Fluid Phase Equilib.* **2004**, *225*, 107–113.
- (17) Soo, C.-B. Experimental Thermodynamic Measurements of Biofuel-related Associating Compounds and Modeling using the PC-SAFT Equation of State. Ph.D. Thesis, MINES ParisTech, Fontainebleau, 2011.
- (18) Janeczek, J.; Paricaud, P. Influence of Cyclic Dimer Formation on the Phase Behavior of Carboxylic Acids. *J. Phys. Chem. B* **2012**, *116*, 7874–7882.
- (19) Sear, R. P.; Jackson, G. Thermodynamic Perturbation Theory for Association into Doubly Bonded Dimers. *Mol. Phys.* **1994**, *82*, 1033–1048.
- (20) Gross, J.; Sadowski, G. Application of the Perturbed-Chain SAFT Equation of State to Associating Systems. *Ind. Eng. Chem. Res.* **2002**, *41*, 5510–5515.
- (21) Gross, J.; Sadowski, G. Perturbed-Chain SAFT: An Equation of State Based on a Perturbation Theory for Chain Molecules. *Ind. Eng. Chem. Res.* **2001**, *40*, 1244–1260.
- (22) Huang, S. H.; Radosz, M. Equation of State for Small, Large, Polydisperse, and Associating Molecules. *Ind. Eng. Chem. Res.* **1990**, *29*, 2284–2294.
- (23) Huang, S. H.; Radosz, M. Equation of State for Small, Large, Polydisperse, and Associating Molecules: Extension to Fluid Mixtures. *Ind. Eng. Chem. Res.* **1991**, *30*, 1994–2005.
- (24) Sear, R. P.; Jackson, G. Thermodynamic Perturbation-Theory for Association into Chains and Rings. *Phys. Rev. E* **1994**, *50*, 386–394.
- (25) Wolbach, J. P.; Sandler, S. I. Using Molecular Orbital Calculations to Describe the Phase Behavior of Cross-Associating Mixtures. *Ind. Eng. Chem. Res.* **1998**, *37*, 2917–2928.
- (26) Wagner, M. MSc Thesis, University Negev (Data from the DDB database), 1979.
- (27) Ameramez, S.; Biarge, F. J. Thermodynamic Behavior of Some Acetic Acid-Alcohol Binary-Systems in Vapor Equilibrium. *An. Quim.* **1973**, *69*, 569–586.
- (28) Miyamoto, S.; Nakamura, S.; Iwai, Y.; Arai, Y. Measurement of Isothermal Vapor-Liquid Equilibria for Binary and Ternary Systems Containing Monocarboxylic Acid. *J. Chem. Eng. Data* **2001**, *46*, 1225–1230.
- (29) Miyamoto, S.; Nakamura, S.; Iwai, Y.; Arai, Y. Measurement of Isothermal Vapor-Liquid Equilibria for Monocarboxylic Acid Plus Monocarboxylic Acid Binary Systems with a Flow-Type Apparatus. *J. Chem. Eng. Data* **2001**, *46*, 405–409.
- (30) Ito, T.; Yoshida, F. Vapor-Liquid Equilibria of Water-Lower Fatty Acid Systems: Water-Formic Acid, Water Acetic Acid and Water-Propionic Acid. *J. Chem. Eng. Data* **1963**, *8*, 315–320.
- (31) Pemberton, R. C.; Mash, C. J. Thermodynamic Properties of Aqueous Non-Electrolyte Mixtures. 2. Vapor-Pressures and Excess Gibbs Energies for Water+Ethanol at 303.15 to 363.15 K Determined by an Accurate Static Method. *J. Chem. Thermodyn.* **1978**, *10*, 867–888.
- (32) Ramalho, R. S.; James, W.; Carnahan, J. F. Effect of Alkaline-Earth Chloride on Vapor-Liquid Equilibrium of Acetic Acid-Water System. *J. Chem. Eng. Data* **1964**, *9*, 215–217.